State-resolved differential and integral cross sections for the reaction $H+D_2 \rightarrow HD(v'=3,j'=0-7)+D$ at 1.64 eV collision energy

Brian D. Bean,[a] James D. Ayers, Félix Fernández-Alonso,[b] and Richard N. Zare
Department of Chemistry, Stanford University, Stanford, California 94305-5080

(Received 30 October 2001; accepted 29 January 2002)

A 212.8 nm laser initiates the reaction $H+D_2 \rightarrow HD+D$ in a mixture of HBr and D_2. A second laser state-selectively ionizes the $HD(v'=3,j')$ reaction product, allowing a determination of the speed distribution and the relative cross section in a velocity-sensitive time-of-flight mass spectrometer. From these measurements we construct differential and integral cross sections for $H+D_2 \rightarrow HD(v'=3,j'=0-7)+D$ at 1.64 ± 0.05 eV collision energy. Although the integral cross sections do not show any unusual features, the differential cross sections reveal forward-scattered features that have not been observed in crossed-beam experiments. An analysis of the scattering features in $HD(v'=3,j'=1-4)$ suggests that these states are dominated by classical hard-sphere scattering. This hard-sphere (direct recoil) mechanism, however, cannot account for the dominant forward scattering observed in $HD(v'=3,j'=0)$. © *2002 American Institute of Physics.*
[DOI: 10.1063/1.1462576]

I. INTRODUCTION

The hydrogen exchange reaction, $H+H_2 \rightarrow H_2+H$, has been the subject of theoretical scrutiny for over 70 years. Consisting of only three nuclei and three electrons, the simplicity of the system has lent itself to innumerable calculations and the production of extremely accurate potential energy surfaces (PES). The most recent PES, the ''Exact Quantum Monte Carlo'' surface of Wu, Kuppermann, and Anderson[1] contains 71 969 points with an accuracy of 0.018 kcal/mol. Such resolution was unthinkable when Eyring and Polanyi published the first H_3 PES (Ref. 2) in 1931. With this and other high accuracy surfaces [LSTH (Refs. 3,4), DMBE (Ref. 5), BKMP2 (Refs. 6,7)] it has been possible to calculate the properties of the hydrogen-atom hydrogen-molecule exchange reaction with unparalleled precision. By forecasting properties that can be experimentally measured (kinetic rates, product branching ratios, angular scattering distributions, stereodynamics) it is possible to probe the nuances of the interaction between three hydrogen atoms. When discrepancies arise between theory and experiment, insight is gained regarding the accuracy of the surfaces, the validity of calculational methods, and the precision of the experiments. It is for this reason that experimental measurements of the hydrogen exchange reaction are crucial to the understanding of this ''simplest'' of all neutral chemical reactions.

The hydrogen exchange reaction does not lend itself to straightforward experimental study. Obstacles include the difficulty of producing well-defined H atoms in the gas phase, a small total cross section for the reaction (~ 1 Å^2), and the wide distribution of rovibrational product states populated by reaction. The difficulty of physically characterizing this reaction has resulted in a body of experimental work that is dwarfed by theoretical studies. However, continued theoretical and experimental refinements have produced a near-exact match between scattering results from quantum mechanical (QM) calculations and high-resolution crossed-beam[8,9] and photoinitiated beam experiments.[10]

Despite this success, questions persist regarding the degree to which quantum mechanical phenomena, such as dynamical resonances[11–20] and the geometric phase,[21–27] play a role in this reaction. These questions have been the impetus for continuing refinements in our ability to study the $H+D_2 \rightarrow HD(v',j')+D$ reaction in the laboratory. We recently reported[28–31] success in the use of photoinitiated methods to simultaneously produce hot H atoms in the presence of deuterium and to detect the HD product scattering in a state-specific manner. While the reported angular resolution is less than that of high-resolution beam experiments, our technique allows us to measure the entire range of scattering angles ($\cos\theta=-1$ to 1), and produce center-of-mass differential cross sections (DCS). In particular, this full-angle capability allows us to probe the forward-scattered region, an area that is rich with dynamical information.

Our previous measurements of $H+D_2 \rightarrow HD(v',j')+D$ probed the $HD(v'=1,2,j')$ products at collision energies dictated by the spectroscopy of the HD $2+1$ resonance enhanced multiphoton ionization (REMPI) transitions used for detection ($E_{coll}=1.53-1.71$ eV). From these DCSs a clear trend emerged; the most probable angle of reactive scattering ($\cos\theta_{mp}$) steadily increases as a function of product rotational state. That is, $j'=0$, 1 products are primarily backscattered whereas higher j' states favor side scattering. Furthermore, a linear relationship was shown to exist between $\cos\theta_{mp}$ and j'^2. This correlation between rotational product state and scattering angle is consistent with a simple, classical model based on specular scattering[32] and the line-of-

[a]Present address: Division of Chemistry and Chemical Engineering, California Institute of Technology, Pasadena, California 91125.
[b]Present address: Istituto di Struttura della Materia, Consiglio Nazionale delle Ricerche, Area della Ricerca di Roma-Tor Vergata, via del Fosso del Cavaliere 100, 00133 Rome, Italy.

centers model[33] and gives predictive power regarding the integral cross sections (ICS) of the products.[31]

As an extension of this work, we have made further improvements to our experimental apparatus, including the incorporation of an independent source for photolysis laser radiation. With this change we can maintain the same collision energy while state-selectively probing different $HD(v', j')$ products. We present here a complete set of DCS and ICS measurements for $H+D_2 \rightarrow HD(v'=3, j'=0-7)+D$ at 1.64 ± 0.05 eV, a collision energy in the middle of our previous measurements. A portion of these measurements, $HD(v'=3, j'=1-4)$ agree with our simple model, suggesting a mechanism rooted in classical mechanics. The identification of significant forward-scattered products for the $HD(v'=3, j'=0,1)$ states, however, marks a departure from this simple model.

II. EXPERIMENTAL SETUP

The experimental setup used for these ICS and DCS measurements is identical to that used for similar measurement of $H+D_2 \rightarrow HD(v'=1,2, j')+D$ near 1.6 eV,[28–31] except for the addition of an independent 212.8 nm photolysis source.

We perform "freeze–pump–thaw" purification on 99.8% hydrogen bromide (HBr) to remove contaminant hydrogen and then dilute with deuterium in a Teflon-lined stainless steel cylinder (1:9 mixture; HBr:D_2). A metering valve is used to maintain a constant pressure (300 Torr) of this reaction mixture behind a pulsed nozzle with a 0.5 mm orifice. The nozzle injects the reaction mixture into the extraction region of a Wiley–McLaren[34] time-of-flight (TOF) mass spectrometer that is operated under space-focusing conditions. The extraction field is 43 V/cm for the DCS measurements and 130 V/cm for the ICS measurements. The gas pulse is nominally 500 μs wide and results in a constant background pressure of 10^{-6} Torr in the chamber, as measured by a nude ion gauge. We have verified that these mild expansion conditions do not produce HBr clusters.[28] The location of the nozzle, approximately 2 cm above the reaction region, ensures single-collision conditions during the reaction. In previous work[19,28] we showed that these conditions result in a rotational temperature of 300 K, a translational temperature of 50 K, and an overall collision energy spread of ± 0.05 eV.

After the precursors have entered the chamber, a linearly polarized, 6 ns pulse of 212.8 nm light (fifth harmonic of an Nd:YAG laser) intersects the sample, photolyzing the HBr to initiate the reaction $H+D_2 \rightarrow HD+D$. This photolysis wavelength produces two sets of H atoms, with kinetic energies of 2.05 eV and 1.60 eV, corresponding to the production of ground-state ($^2P_{3/2}$) and spin-excited-state ($^2P_{1/2}$) bromine. Conservation of energy limits the H-atoms from the excited channel to the production of $HD(v'=2, j'=8)$ and lower rovibrational states. Because we only measure the $HD(v'=3, j')$ products in this study, we can ignore the photolysis channel that produces ($^2P_{1/2}$) bromine. The H-atoms from the ($^2P_{3/2}$) bromine channel have an anisotropy of $\beta=-1$ as a result of the perpendicular character ($\Delta\Omega=\pm 1$) of this transition.[28,35]

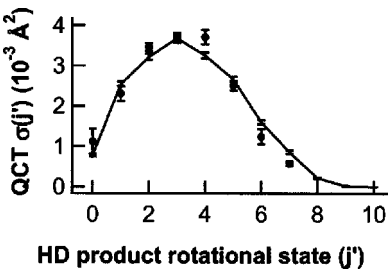

FIG. 1. Measured distribution of $HD(v'=3,j')$ product states (ICS) and comparison to QCT calculations for the $H+D_2 \rightarrow HD+D$ reaction at 1.64 eV. Filled circles are experimental points and the solid line represents theoretical calculations; error bars give 90% confidence intervals on experimental points. The area under the experimental curve has been normalized to the area under the QCT curve. (Ordinate axis corresponds to QCT calculations.)

After approximately 15 ns of reaction time, a counter-propagating laser pulse enters the chamber and selectively ionizes the $HD(v'=3, j')$ state of interest. We use a $2+1$ REMPI process via the HD $EF\ ^1\Sigma_g^+ - X\ ^1\Sigma_g^+$ transition that requires tunable laser light from 224 to 227 nm. This wavelength range is obtained by mixing doubled light from a dye laser with residual 1064 nm light from the Nd:YAG pump laser. The resulting "probe" pulse has a temporal width of 6 ns, and a set of thin-film polarizers attenuates it to ~ 300 μJ before it enters the chamber. Upon ionization, the HD^+ from the rovibrational state of interest is accelerated through the TOF assembly to strike a microchannel plate detector, creating a signal that is collected with a digital oscilloscope.

The linewidth of the resulting probe beam (0.4 cm^{-1}) is narrower than the Doppler width of the HD products arising from their speed in the laboratory (up to 6.7 km/s). When measuring a distribution of $HD(v'=3, j')$ product states (integral cross section) we scan the probe wavelength through the REMPI transition to ensure that we sample the full range of product speeds along the laser axis.[31] The area of these signal vs wavelength plots are a direct measurement of the relative populations of the $HD(v'=3, j')$ products for this reaction as the REMPI line strengths have been shown to be nearly identical.[36,37]

When making DCS measurements, we reduce the voltage in the TOF to allow the HD products to spread out spatially, ultimately improving our angular resolution. As the ion packet spreads out, however, our signal shrinks in comparison to the noise. To counter this effect we employ an ion-counting scheme whereby only ions striking the detector within a predetermined time frame, and with a magnitude corresponding to a single ion, are counted as signal. Additionally, the ion packet is "core-extracted"[28,38] before it strikes the detector to simplify the conversion from the TOF profile (see Fig. 2) to the DCS (see Fig. 3). The marked reduction in signal from our core-extraction technique necessitates $\geqslant 20\,000$ laser shots to produce the profiles shown in Fig. 2. Because the wavelengths necessary to cause two-photon excitation of the HD $EF\ ^1\Sigma_g^+ - X\ ^1\Sigma_g^+$ (0, 3) band result in a center-of-mass collision energy of 1.39 eV or less, there was no measurable "prompt" (i.e., probe-induced) signal. Thus, it was unnecessary to perform a shot-to-shot subtraction as had been done previously.[39]

TABLE I. Lab-frame speed ranges of products from the reaction $H+D_2 \rightarrow HD(v'=3,j')+D$ at 1.64 eV collision energy as dictated by conservation of energy and linear momentum in the center-of-mass frame. A greater range of speeds justifies more basis functions in our fitting algorithm, which translates into more points in the differential cross section (see Fig. 3).

Rotational state (j')	Forward-scattered limit (m/s)	Backward-scattered limit (m/s)	Basis functions
0	6617	1302	8
1	6517	1348	8
2	6476	1443	6
3	6327	1592	6
4	6116	1803	6
5	5822	2098	4
6	5399	2521	4
7	4645	3274	4

The speed of $HD(v'=3,j')$ products in the laboratory (Table I) makes the focus and alignment of the lasers critical. The photolysis laser is intentionally focused 3 cm before the pulsed-jet expansion to produce a reaction volume with a cross section of $\sim 1\ mm^2$. The focus of the probe laser is then positioned within this reaction volume. If the probe beam is not centered, the distribution of HD speeds measured will not be representative of the reaction. Fortunately, if the ionization pulse is sampling the edges of the photolysis volume, the resulting TOF profile is noticeably asymmetric. With small adjustments of the photolysis alignment to produce symmetric TOF profiles we avoid missing the fastest moving products.

The measured TOF profiles are converted into DCSs using a law-of-cosines analysis, the so-called photoloc technique.[40] The TOF signal is fit by use of a singular-value decomposition (SVD) algorithm and then refit with a simulated annealing/maximum entropy algorithm as a further consistency check.[28] Both methods give very similar results.

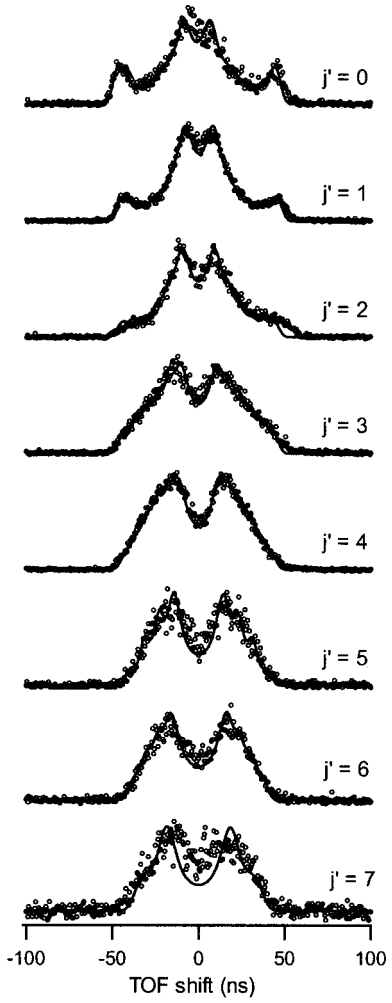

FIG. 2. Core-extracted time-of-flight profiles for $H+D_2 \rightarrow HD(v'=3,j')+D$ at 1.64 eV collision energy. Open circles are experimental points and solid lines are SVD fits to the data. Each profile corresponds to 20 000 or more laser shots. See text for an explanation of the TOF shift.

III. RESULTS

Figure 1 compares the measured distribution of $HD(v'=3,j')$ states from the reaction $H+D_2 \rightarrow HD+D$ at 1.64 eV collision energy to QCT calculations.[19] The experimental distribution has been normalized to the area of the QCT calculation for comparison. Each point represents at least three measurements, and the error bars correspond to a 90% confidence interval. The correspondence between experiment and QCT calculations is quite good, and the overall shape of the distribution resembles other ICS measurements for this reaction.[8,9,31,41–43] The ordinate axis, corresponding to the QCT calculations, emphasizes the small cross section for reaction into the $v'=3$ vibrational manifold at 1.64 eV collision energy. For the reaction $H+D_2 \rightarrow HD(v'=3,j'=0)+D$, for example, QCT calculations suggest a cross section for reaction on the order of 1×10^{-3} Å^2.

Figure 2 presents the core-extracted TOF profiles for the eight energetically available $HD(v'=3)$ rotational product states. The solid line is the SVD fit to the experimental points, shown as open circles. Each TOF profile represents the distribution of HD^+ ions striking the detector relative to the arrival time of HD^+ ions that have no speed in the laboratory (TOF shift=0 ns). Negative TOF shifts correspond to HD products that were originally moving toward the detector before ionization, and positive TOF shifts correspond to HD products originally moving away from the detector. The absolute magnitude of the shift reveals the direction of scattering in the center-of-mass frame; large magnitudes in TOF shifts correspond to forward-scattered products, and small magnitudes correspond to backward-scattered products. Because of conservation of energy, the states presented should have *no* product ions that arrive at TOF shift=0 ns. The appearance of some product signal at TOF shift=0 ns is the result of the finite temporal width of the probe laser and the lack of perfect core extraction (e.g., our instrumental resolution).[28,38]

Because of the kinematics of the experiment, the *size* of an ion peak is not directly proportional to the magnitude of the scattering in the DCS. For the same amount of scattering into some solid angle, forward-scattered signals are much smaller than backward-scattered signals because increased off-axis lab speeds result in the ions being blocked from the detector by the core-extraction mask. This bias is well illustrated by the data for the $HD(v'=3,j'=0)$ product state,

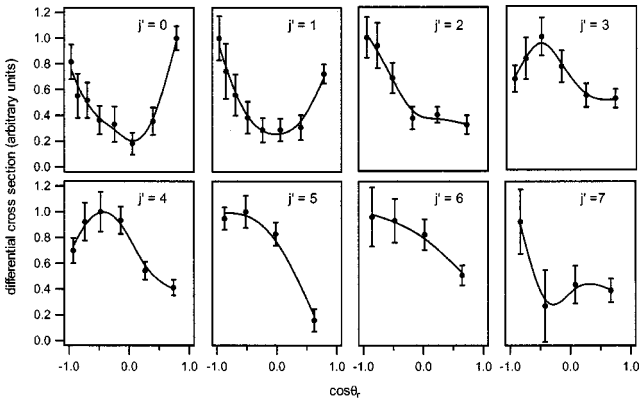

FIG. 3. Differential cross sections for H+D$_2$→HD($v'=3, j'$)+D at 1.64 eV collision energy. Filled circles are SVD fits of data in Fig. 3, and solid lines are spline fits to aid in visualization of scattering. Error bars represent a convolution of random error introduced by the SVD fitting procedure and the estimated experimental (systematic) error. The decreasing number of points from $j'=0$ to $j'=7$ is explained by a decreasing dynamic range of product laboratory speeds.

where small peaks at large TOF shifts correspond to substantial scattering in the forward direction. Furthermore, the most forward-scattered point in the DCS gives little insight as to the sharpness ($\Delta \cos\theta$) of scattering as the angular uncertainty is approximately 30°. When comparing experimental measurements to calculations, however, the decreased resolution of the forward-scattered products can be accommodated by forward-convolution of theoretical DCSs into TOF profiles.[10]

The dramatic change in DCS with rotational product state can be seen in the raw TOF data. The smaller peaks on the wings of the TOF profiles for $j'=0$, 1 can only be the result of forward-scattered reactive product. Moving to higher rotational product states, the forward scattered peaks disappear, giving way to TOF profiles that are primarily backward- to side-scattered. The change in width of the profiles is the consequence of reduced product speeds as product kinetic energy is exchanged for internal rotational energy. Table I shows the change in the physically allowed range of lab speeds for a given product state. As the range of speeds shrinks, we must reduce the number of basis functions in the fitting routine to minimize covariance. The change in basis functions results in a reduction in the number of points in the DCS for the higher rotational levels.

The product-state-resolved DCSs for the title reaction are shown in Fig. 3. The filled circles are the results of the SVD fitting procedure, and the error bars are a convolution of the random error introduced by the SVD fitting procedure and the estimated systematic error from three or more measurements for each rovibrational state. A spline fit has been drawn to aid in visualization of scattering trends. The remarkable forward scattering in the $j'=0$, 1 rotational states has been reported previously,[19] and is theorized to be the result of a scattering resonance in the vicinity of 1.64 eV collision energy. Disregarding the forward-scattered peaks, we see the same trend in scattering previously reported for this reaction,[8,9,29,30,41] the peak of the DCS marches from backward- to side-scattered as a function of rotational product state. The dip in the $j'=7$ DCS is not consistent with this trend, but may be the result of some near-threshold effect as this state is barely accessible at 1.64 eV collision energy.

IV. DISCUSSION

A. Comparison to $v'=1$, 2 measurements near 1.6 eV

In previous works[28–30] we presented DCS measurements for the reaction H+D$_2$→HD+D for the HD($v'=1, j'=1,5,8$) and HD($v'=2, j'=0,3,5$) product states using a single laser that served both as photolysis and probe. Because of the variation in photolysis energy necessitated by HD(v', j') state-selection, the collision energy of the reactions varied from 1.53 eV ($v'=2, j'=5$) to 1.71 eV ($v'=1, j'=1$). In these reactions we reported a linear relationship between the peak of the DCS ($\cos\theta_{mp}$) and the square of the product state (j'^2) for each vibrational manifold. Using a simple hard-sphere model, we showed that the observed behavior is consistent with specular scattering obeying the deflection function,

$$\cos\theta = 2\frac{b^2}{d^2} - 1, \tag{1}$$

where θ is the center-of-mass scattering angle measured from the H-atom direction, b is the impact parameter, and d is the hard sphere radius. We also found that a direct correlation exists between final rotational state (j') and impact parameter (b) via the initial orbital angular momentum ($l=\mu v b$),[44]

$$j' = \alpha l. \tag{2}$$

In a later work[31] we showed that this hard-sphere model also fits the DCSs for H+D$_2$→HD($v'=0,1,2, j'$)+D at 1.28 eV as reported by Welge and co-workers.[8]

In Fig. 4(a) we plot $\cos\theta_{mp}$ versus j'^2 for the reaction H+D$_2$→HD($v'=3, j'$)+D at 1.64 eV. It is noteworthy that the scattering of the HD($v'=3, j'$) states do not follow our hard-sphere model at this energy. The forward-scattered nature of the HD($v'=3, j'=0$) DCS is wholly incompatible with specular scattering (see below), while the DCSs of HD($v'=3, j'=5,6,7$) are more backward-scattered than our model predicts. Nevertheless, there is a trend in $\cos\theta_{mp}$ from backward-scattered for HD($v'=3, j'=1$) to side-scattered for HD($v'=3, j'=4$) that allows for a straight line with slope $m=0.0401$, which is drawn in Fig. 4(a). This line is reproduced in Fig. 4(b) for comparison to the slopes for HD($v'=1, j'$) and HD($v'=2, j'$) at similar collision energies. As was also seen in the 1.28 eV collision energy data of Welge and co-workers, the slopes increase as a function of v'. This trend suggests a smaller effective hard-sphere radius for higher vibrational product states, in agreement with the line-of-centers model.[30,33]

Additionally, the slope of the line in Fig. 4(a) can be used to predict a maximum possible rotational product state, j'_{max}, using the angle-dependent barrier to reaction of the LSTH potential energy surface.[3,4,45] Following the line-of-centers argument presented previously,[29,30] the rotational product states of this reaction at 1.64 eV collision energy, should not exceed $j'_{max}=6$. Furthermore, we may take this

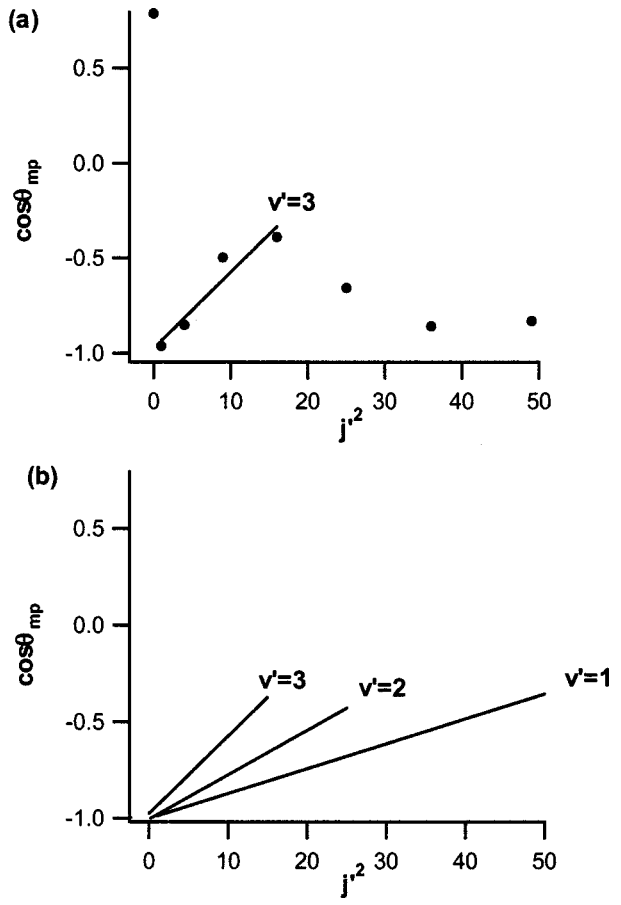

FIG. 4. Plots of cos θ_{mp} vs j'^2. (a) For the $v'=3, j'$ data presented in this work, the slope of the line between $j'=1$ and $j'=4$ is 0.040, resulting in a predicted $j'_{max}=6$ according to a simple hard-sphere specular scattering model. (b) The slopes for HD($v'=1, j'$) and HD($v'=2, j'$) at collision energies near 1.6 eV are also shown for comparison. The slope for the $v'=1$ line is 0.013 resulting in a predicted $j'_{max}=12$, whereas the slope for the $v'=2$ line is 0.023 resulting in a predicted $j'_{max}=9$ (see Refs. 28 and 29).

j'_{max} and produce a plot of product state population vs reduced rotational state ($j'_{red}=j'/j'_{max}$), as shown in Fig. 5. This treatment produces an inverted parabolic distribution similar to that in $H+D_2 \rightarrow HD(v'=0-2, j')+D$ at other

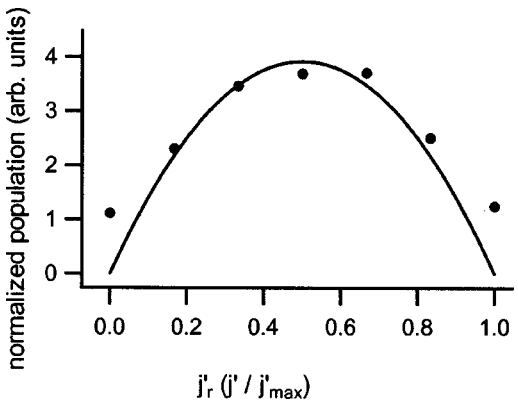

FIG. 5. Plot of rotational state population vs reduced rotational state, $j'_{red}=j'/j'_{max}$. The solid line is the prediction of a simple hard-sphere, specular scattering model in which a linear opacity function is assumed.

collision energies.[31] The solid line shown in Fig. 5 represents the functional form,

$$\sigma(j'_{red}) = c j'_{red}(1-j'_{red}) \tag{3}$$

that results from an opacity function that varies linearly with $1-b/d$.[31] This behavior is a straightforward consequence of a preferentially collinear reaction; collisions with an impact parameter $b=0$ (along the D_2 bond axis) will be most likely to lead to products whereas larger impact parameters will be less likely to react, with no reaction for $b \geqslant d$.

It is not clear at this time whether the discrepancies in HD($v'=3, j'=5-7$) result from a lack of experimental angular resolution or the breakdown of our simple model. Certainly the presence of $j'=7$ products, beyond the predicted $j'_{max}=6$ cutoff indicates that we have oversimplified the dynamics. Nevertheless, it is useful to compare this set of DCS measurements with previously published results, which suggest that the $H+D_2$ reaction can be regarded as primarily governed by hard-sphere scattering.

B. Forward-scattered products

The most significant features of the DCSs in Fig. 3 are the prominent forward scatter in the HD($v'=3, j'=0$) products and, to a lesser extent, the HD($v'=3, j'=1$) products. Forward-scattered products in $H+D_2 \rightarrow HD+D$ (and its isotopic variants) have been predicted by quantum mechanical calculations for over 10 years,[9,25,46–48] but previous measurements of this system with crossed-molecular beam experiments[8,9,41,49–53] could not observe the forward scattered region because of kinematic constraints. While early ion-imaging measurements[54] showed backscattered D-atom products (forward HD products) from this reaction in the total (summed over all states) DCS, the present work is, to our knowledge, the first experimental observation of this feature on a state-selective basis.

The forward-scattered peak in the HD($v'=3, j'=0$) products has been the subject of recent discussion. As we reported,[19] QCT calculations on the BKMP2 PES produce a differential cross section for HD($v'=3, j'=0$) which has at least twice as much backward-scattered products as forward-scattered products. This quasiclassical result is in obvious disagreement with Fig. 3, where the forward-scattered peak for HD($v'=3, j'=0$) *exceeds* the backward scattered peak. Supported by opacity function and time delay calculations,[19] we have suggested that the forward scattered products might be the result of a scattering resonance. Calculations by Truhlar and co-workers,[55] who used a locally vibrationally adiabatic model, predict that a resonance does exist for the HD($v'=3, j'=0$) product state at 1.83 eV total energy (center-of-mass collision energy $=1.64$ eV), but recent quantum mechanical calculations by Kendrick[20] call into question this resonance interpretation. Whatever its exact nature, it seems to us inescapable that this behavior is quantum mechanical in origin.

V. CONCLUSIONS

We have used a photoinitiated reaction technique to make reactive scattering measurements on the $H+D_2$

$\rightarrow HD(v'=3, j'=0-7)+D$ reaction at 1.64 eV collision energy. Despite the small cross section for reaction into these states ($\sim 1\times 10^{-3}$ Å^2), we have made DCS measurements that span the full angular range. Analysis of the angular scattering, as well as the product state distributions, suggests that this reaction is primarily the result of (previously observed) classical mechanisms. Although contributing much less to the overall reaction cross section, we find dramatic forward scattering in the $HD(v'=3, j'=0)$ DCS. To a lesser extent forward scattering is also present in the $HD(v'=3, j'=1)$ DCS. In both cases the amount of forward scattering is larger than what would be expected from a quasiclassical treatment of this reaction process. We have suggested that this behavior might be a signature of some scattering resonance, but a definitive interpretation must await more reliable fully quantum mechanical calculations.

ACKNOWLEDGMENTS

B.D.B. thanks Elf-Atochem for graduate fellowship support and J.D.A. thanks the Hertz Foundation for graduate fellowship support. F.F.A. acknowledges partial financial support in the form of a Marie Curie Fellowship of the European Program ''Improving Human Research Potential and the Socio-Economic Knowledge Base'' under Contract No. HPMFCT-2000-00683. L. Bañares and F. J. Aoiz are acknowledged for their assistance with the QCT code and for useful discussions. We are also grateful to A.E. Pomerantz for a critical proofreading of the manuscript. This work was supported by the National Science Foundation under Grant No. CHE-99-00305.

[1] Y.-S. M. Wu, A. Kuppermann, and J. B. Anderson, Phys. Chem. Chem. Phys. **1**, 929 (1999).
[2] H. Eyring and M. Polanyi, Z. Phys. Chem. Abt. B **12**, 279 (1931).
[3] P. Siegbahn and B. Liu, J. Chem. Phys. **68**, 2457 (1978).
[4] D. G. Truhlar and C. J. Horowitz, J. Chem. Phys. **68**, 2466 (1978).
[5] A. J. C. Varandas, F. B. Brown, C. A. Mead, D. G. Truhlar, and N. C. Blais, J. Chem. Phys. **86**, 6258 (1987).
[6] A. I. Boothroyd, W. J. Keogh, P. G. Martin, and M. R. Peterson, J. Chem. Phys. **95**, 4343 (1991).
[7] A. I. Boothroyd, W. J. Keogh, P. G. Martin, and M. R. Peterson, J. Chem. Phys. **104**, 7139 (1996).
[8] L. Schnieder, K. Seekamp-Rahn, E. Wrede, and K. H. Welge, J. Chem. Phys. **107**, 6175 (1997).
[9] E. Wrede, L. Schnieder, K. H. Welge, F. J. Aoiz, L. Bañares, F. J. Castillo, B. Martínez-Haya, and V. J. Herrero, J. Chem. Phys. **110**, 9971 (1999).
[10] F. Fernández-Alonso, B. D. Bean, R. N. Zare, F. J. Aoiz, L. Bañares, and J. F. Castillo, J. Chem. Phys. **115**, 4534 (2001).
[11] R. D. Levine and S.-F. Wu, Chem. Phys. Lett. **11**, 557 (1971).
[12] D. G. Truhlar and A. Kuppermann, J. Chem. Phys. **56**, 2232 (1972).
[13] G. C. Schatz and A. Kuppermann, J. Chem. Phys. **59**, 964 (1973).
[14] A. Kuppermann, in *Potential Energy Surfaces and Dynamics Calculations*, edited by D. G. Truhlar (Plenum, New York, 1981), p. 375.
[15] J.-C. Nieh and J. J. Valentini, Phys. Rev. Lett. **60**, 519 (1988).
[16] R. Sadeghi and R. T. Skodje, J. Chem. Phys. **99**, 5126 (1993).
[17] S. Kennedy, K. Dharmesena, S. Moser, M. Auzinsh, and N. E. Shafer-Ray, Chem. Phys. **244**, 449 (1999).
[18] B. K. Kendrick, L. Jayasinghe, S. Moser, M. Auzinsh, and N. Shafer-Ray, Phys. Rev. Lett. **84**, 4325 (2000); **86**, 2482 (2001).
[19] F. Fernández-Alonso, B. D. Bean, J. D. Ayers, A. E. Pomerantz, R. N. Zare, L. Bañares, and F. J. Aoiz, Angew. Chem. Int. Ed. Engl. **2000**, 2748 (2000).
[20] B. K. Kendrick, J. Chem. Phys. **114**, 8796 (2001).
[21] Y.-S. M. Wu, A. Kuppermann, and B. Lepetit, Chem. Phys. Lett. **186**, 319 (1991).
[22] Y.-S. M. Wu and A. Kuppermann, Chem. Phys. Lett. **201**, 178 (1993).
[23] A. Kuppermann and Y.-S. M. Wu, Chem. Phys. Lett. **205**, 577 (1993).
[24] A. Kuppermann and Y.-S. M. Wu, Chem. Phys. Lett. **241**, 229 (1995).
[25] Y.-S. M. Wu and A. Kuppermann, Chem. Phys. Lett. **235**, 106 (1995).
[26] E. Wrede, L. Schnieder, K. H. Welge, F. J. Aoiz, L. Bañares, V. J. Herrero, B. Martínez-Haya, and V. S. Rábanos, J. Chem. Phys. **106**, 7862 (1997).
[27] B. K. Kendrick, J. Chem. Phys. **112**, 5679 (2000).
[28] F. Fernández-Alonso, B. D. Bean, and R. N. Zare, J. Chem. Phys. **111**, 1022 (1999).
[29] F. Fernández-Alonso, B. D. Bean, and R. N. Zare, J. Chem. Phys. **111**, 1035 (1999).
[30] F. Fernández-Alonso, B. D. Bean, and R. N. Zare, J. Chem. Phys. **111**, 2490 (1999).
[31] B. D. Bean, F. Fernández-Alonso, and R. N. Zare, J. Phys. Chem. A **105**, 2228 (2001).
[32] G. H. Kwei and D. R. Herschbach, J. Phys. Chem. **83**, 1550 (1979).
[33] I. W. M. Smith, J. Chem. Educ. **59**, 9 (1982).
[34] W. C. Wiley and I. H. McLaren, Rev. Sci. Instrum. **26**, 1150 (1955).
[35] P. M. Regan, S. R. Langford, A. J. Orr-Ewing, and M. N. R. Ashfold, J. Chem. Phys. **110**, 281 (1999).
[36] W. M. Huo, J. Chem. Phys. **95**, 205 (1991).
[37] K.-D. Rinnen, M. A. Buntine, D. A. V. Kliner, and R. N. Zare, J. Chem. Phys. **95**, 214 (1991).
[38] W. R. Simpson, A. J. Orr-Ewing, T. P. Rakitzis, S. A. Kandel, and R. N. Zare, J. Chem. Phys. **103**, 7299 (1995).
[39] H. Xu, N. E. Shafer-Ray, F. Merkt, D. J. Hughes, M. Springer, R. P. Tuckett, and R. N. Zare, J. Chem. Phys. **103**, 5157 (1995).
[40] N. E. Shafer, A. J. Orr-Ewing, W. R. Simpson, H. Xu, and R. N. Zare, Chem. Phys. Lett. **212**, 155 (1993).
[41] L. Bañares, F. J. Aoiz, V. J. Herrero, M. J. D'Mello, B. Niederjohann, K. Seekamp-Rahn, E. Wrede, and L. Schnieder, J. Chem. Phys. **108**, 6160 (1998).
[42] K.-D. Rinnen, D. A. V. Kliner, and R. N. Zare, J. Chem. Phys. **91**, 7514 (1989).
[43] K.-D. Rinnen, D. A. V. Kliner, R. S. Blake, and R. N. Zare, Chem. Phys. Lett. **153**, 371 (1988).
[44] I. R. Elsum and R. G. Gordon, J. Chem. Phys. **76**, 3009 (1982).
[45] R. D. Levine and R. B. Bernstein, Chem. Phys. Lett. **105**, 467 (1984).
[46] R. E. Continetti, J. Z. H. Zhang, and W. H. Miller, J. Chem. Phys. **93**, 5356 (1990).
[47] W. H. Miller and J. Z. H. Zhang, J. Phys. Chem. **95**, 12 (1991).
[48] F. J. Aoiz, L. Bañares, M. J. D'Mello, V. J. Herrero, V. S. Rábanos, L. Schnieder, and R. E. Wyatt, J. Chem. Phys. **101**, 5781 (1994).
[49] E. Wrede and L. Schnieder, J. Chem. Phys. **107**, 786 (1997).
[50] L. Schnieder, K. Seekamp-Rahn, H. Steuwe, and K. H. Welge, Faraday Discuss. Chem. Soc. **91**, 259 (1991).
[51] R. E. Continetti, B. A. Balko, and Y. T. Lee, J. Chem. Phys. **93**, 5719 (1990).
[52] S. A. Buntin, C. F. Giese, and W. R. Gentry, J. Chem. Phys. **87**, 1443 (1987).
[53] S. A. Buntin, C. F. Giese, and W. R. Gentry, Chem. Phys. Lett. **168**, 513 (1990).
[54] T. N. Kitsopoulos, M. A. Buntine, D. P. Baldwin, R. N. Zare, and D. W. Chandler, Science **260**, 1605 (1993).
[55] T. C. Allison, R. S. Friedman, D. J. Kauffman, and D. G. Truhlar, Chem. Phys. Lett. **327**, 439 (2000).